Talanta 78 (2009) 1401–1407

Contents lists available at ScienceDirect

Talanta

journal homepage: www.elsevier.com/locate/talanta

An amperometric urea biosensor based on covalently immobilized urease on an electrode made of hyperbranched polyester functionalized gold nanoparticles

Ashutosh Tiwari [a], Santosh Aryal [a], Srikanth Pilla [a], Shaoqin Gong [a,b,*]

[a] Department of Mechanical Engineering, University of Wisconsin-Milwaukee, 3200 North Cramer Street, Milwaukee, WI 53211, USA
[b] Department of Materials, University of Wisconsin-Milwaukee, 3200 North Cramer Street, Milwaukee, WI 53211, USA

ARTICLE INFO

Article history:
Received 17 January 2009
Received in revised form 12 February 2009
Accepted 13 February 2009
Available online 26 February 2009

Keywords:
Urea biosensor
Amperometric detection
Covalent immobilization
Boltron® H40
Gold nanoparticles

ABSTRACT

An amperometric biosensor was fabricated for the quantitative determination of urea in aqueous medium using hematein, a pH-sensitive natural dye. The urease (Urs) was covalently immobilized onto an electrode made of gold nanoparticles functionalized with hyperbranched polyester-Boltron® H40 (H40–Au) coated onto an indium–tin oxide (ITO) covered glass substrate. The covalent linkage between the Urs enzyme and H40–Au nanoparticles provided the resulting enzyme electrode (Urs/H40–Au/ITO) with a high level of enzyme immobilization and excellent lifetime stability. The response studies were carried out as a function of urea concentration with amperometric and photometric measurements. The biosensor based on Urs/H40–Au/ITO as the working electrode showed a linear current response to the urea concentration ranging from 0.01 to 35 mM. The urea biosensor exhibited a sensitivity of 7.48 nA/mM with a response time of 3 s. The Michaelis–Menten constant for the Urs/H40–Au/ITO biosensor was calculated to be 0.96 mM, indicating the Urs enzyme immobilized on the electrode surface had a high affinity to urea.

1. Introduction

Kidneys perform key roles in various body functions, including excreting metabolic waste products such as urea from the bloodstream, regulating the hydrolytic balance of the body, and maintaining the pH of body fluids [1]. The level of urea in blood serum is the best measurement of kidney function and staging of kidney diseases [2]. The normal urea level in serum ranges from 15 to 40 mg/dL (i.e., 2.5–7.5 mM). An increase in urea concentration causes renal failure such as acute or chronic urinary tract obstruction with shock, burns, dehydration, and gastrointestinal bleeding, whereas a decrease in urea concentration causes hepatic failure, nephritic syndrome, and cachexia [3]. Therefore, there is an urgent need to develop a device that rapidly monitors urea concentration in the body.

Most existing urea biosensors utilize urease (Urs) as the sensing element. The available Urs on the electrode surface hydrolyzes urea into NH_4^+ and HCO_3^- ions [4]. The concentration of urea is measured by monitoring the librated ions using a transducer such as amperometric, potentiometric, optical, thermal, or piezoelectric [5–11]. Although various urea biosensors that use a range of transducers have been studied extensively, the Urs-based amperometric urea biosensor is considered one of the most promising approaches because it offers fast, simple, and low-cost detection. The response time of such a biosensor is directly associated with the hydrolysis rate of urea on the electrode surface; therefore, rapid production of NH_4^+ ions on the electrode will lead to a highly sensitive biosensor.

It is well established that the performance of biosensors greatly depends on the physicochemical properties of the electrode materials, enzyme immobilization procedure, and enzyme concentration on the electrode surface [12]. Many electrode materials have been used to fabricate urea biosensors such as bovine serum albumin embedded polypyrrole [13]; polyvinyl alcohol–polyacrylamide composite [14]; amine functionalized glassy carbon [15]; polyvinylferrocenium [16]; poly(*N*-3-aminopropylpyrrole)-*co*-pyrrole [17]; polyaniline–Nafion®/Au composite [18]; polyethylenimine [19]; poly(*N*-vinyl carbazole)/stearic acid [20]; polyaniline–poly(n-butyl methacrylate) composites [21]; chitosan [22]; and polyaniline–perfluorosulfonated ionomer composite [5]. However, there is an ongoing demand for new types of electrode materials that can provide the Urs enzyme with better stability and performance for *in vitro* urea measurement.

In this context, the use of nanomaterials to fabricate biosensors is one of the most exciting approaches because nanomaterials have a unique structure and high surface-to-volume ratio [23]. The surfaces of nanomaterials can also be tailored in the molecular scale in order to achieve various desirable properties [24]. Many

* Corresponding author at: Department of Mechanical Engineering, University of Wisconsin-Milwaukee, 3200 North Cramer Street, Milwaukee, WI 53211, USA. Tel.: +1 414 229 5946; fax: +1 414 229 6958.
E-mail address: sgong@uwm.edu (S. Gong).

0039-9140/$ – see front matter © 2009 Elsevier B.V. All rights reserved.
doi:10.1016/j.talanta.2009.02.038

attempts have been made to fabricate a third-generation biosensor with self-assembly technology [25–31]; however, these approaches were based on planar self-assembly that may only offer limited available surface area on the electrode, which can compromise the performance of the biosensor.

Meanwhile, gold nanoparticles have played an increasingly important role for biosensor applications over the last decade [29,30]. Gold nanoparticles can (1) provide a stable surface for the immobilization of biomolecules without compromising their biological activities and (2) permit direct electron transfer from the redox biomolecules to the bulk electrode materials, thereby enhancing the electrochemical sensing ability [29]. For example, Shipway et al. systematically studied the new electronic, photoelectronic, and sensoring systems that used gold nanoparticle superstructures on the electrode surface [30]. In addition, previous studies indicated that biological macromolecules such as enzymes can generally retain their enzymatic and electrochemical activity after being immobilized onto the gold nanoparticles [32,33].

This study investigates the feasibility of using gold nanoparticles functionalized with hyperbranched polyester, Boltorn® H40 (H40–Au), for a potential urea biosensing application. H40–Au nanoparticles are particularly attractive for biosensor fabrication because they can be prepared under ambient conditions and they exhibit tunable porosity, high thermal stability and chemical inertness while experiencing negligible swelling in aqueous solution. In this work, successful attempts have been made toward the fabrication of an efficient urea biosensor using H40–Au nanoparticles. This novel urea biosensor offers a relatively long shelf life, a broad detection range, a high sensitivity, and a short response time.

2. Experimental

2.1. Materials

Boltorn® H40 (64 hydroxyl groups per molecule and M_n of 2833) was provided by Perstorp Polyols, Inc. and used after purification. The following materials were used without further purification: 3-mercaptopropionic acid (Aldrich, 99%), sodium borohydride (Aldrich, 99%), hydrogen tetrachloroaurate (III) hydrate (Aldrich, 99.99%), 1-ethyl-3-(3-dimethylaminopropyl) carbodiimide hydrochloride (Aldrich, 99%), *N*,*N*′-dicyclohexylcarbodiimide (Aldrich, 99%), *N*-hydroxysuccinimide (Aldrich, 99%), hematein (Fluka, 98%), L-serine (Acros, 99%), L-threonine (Acros, 98%), α-ketoglutaric acid (Fluka, 98%), L-alanine (Acros, 99%), L-phenylalanine (Acros, 98.5%), uric acid (Acros, 99%), L-cystine (Acros, 99%), L (+)-glutamic acid (Acros, 99%) sodium pyruvate (Fisher, 99%), L-glutamine (Fisher, 98.5%), L-ascorbic acid (Fisher, 99.8%), urea (Acros, 99%) and urease (Aldrich, from *Canavalia ensiformis*). All supplementary chemicals were of analytical grades and solutions were prepared with 18.2 MΩ deionized water. Indium–tin oxide (ITO) coated glass sheets (Balzers) with a resistance of 15 Ω/cm^2 were used as substrates for the deposition of electrodes.

2.2. Functionalization of gold nanoparticles with hyperbranched polyester

Functionalization of gold nanoparticles with hyperbranched polyester was conducted via a two-step procedure. First, the gold nanoparticle was functionalized with mercapto propionic acid (Au–COOH). Next, amine functionalized hyperbranched Boltorn® H40 (H40–NH_2) was covalently grafted onto Au–COOH nanoparticles using *N*,*N*′-dicyclohexylcarbodiimide (DCC) and *N*-hydroxysuccinimide (NHS) mediated reaction [34].

2.2.1. Preparation of carboxyl functionalized gold (Au–COOH) nanoparticles

To prepare the Au–COOH nanoparticles, concentrated solutions of tetrachloroauric acid ($HAuCl_4$) and 3-mercaptopropionic acid (MPA) were first prepared in ethanolic acetic acid, 0.001 M. Next, 10 mL of a solution containing 6 mM $HAuCl_4$ and 12 mM MPA was prepared by diluting the concentrated stock solutions with ethanol. All solutions were prepared fresh prior to reduction. Reduction was carried out by adding 65 μL of a 1.4 M aqueous solution of sodium borohydride ($NaBH_4$) in 5 μL portions under constant stirring. To form stable thiol monolayers on the gold nanoparticles, the suspension was allowed to stir slowly overnight in a dark at room temperature for 24 h. After that, the gold suspension was placed into an eppendorf tube and washed three times (centrifugation at 5000 rpm for 25 min) with ethanol to remove excess alkanethiol from the suspension.

2.2.2. Preparation of amine functionalized Boltorn® H40 (H40–NH_2)

First, 1.5 mL hydrazoic acid (1 M) was added into 20 mL Boltorn® H40 solution (5%, w/v in THF) and then mixed at room temperature. In this mixture, 0.3 mL diisopropyl azodicarboxylate (1.5 mM) and 5 mL triphenylphosphine (3.0 mM) were added under continuous stirring. After 1 h, the reaction mixture was heated to 50 °C and kept for 3 h; after which 1 mL HCl (1N) was added drop wise. The reaction then continued for additional 3 h. Finally, the reaction products were cooled to room temperature, filtered, and dried under vacuum.

2.2.3. Grafting H40–NH_2 onto the Au–COOH nanoparticles

H40–NH_2 was grafted onto Au–COOH using DCC and NHS as the condensing agents at room temperature (Fig. 1A). In a typical experiment, 50 mg of Au–COOH was dissolved in 10 mL DMSO and activated with 0.3 mM of DCC and NHS at room temperature. Next, 1 g of H40–NH_2 dissolved in 40 mL THF was added to the solution and the resulting solution mixture was stirred for 24 h. After that, the solution mixture was filtered to remove any insoluble byproducts, residual impurities, and aggregates. The final product was recovered by precipitation with cold diethylether and dried under vacuum.

2.3. Preparation of the Au–H40/ITO electrode

Ten microlitres of 2% (w/v) H40–Au nanoparticle solution in $CHCl_3$ was uniformly spread on the ITO substrate by drop coating technique at room temperature (Fig. 1B). The H40–Au/ITO electrode was dried under vacuum.

2.4. Fabrication of the urea bioactive electrode

The urea bioactive electrode was prepared by covalent immobilization of the urea-specific enzyme, urease, over the H40–Au/ITO electrode. In order to immobilize Urs, the H40–Au/ITO electrode was immersed in a phosphate buffer solution (1 M, pH 7.0) containing previously activated Urs enzyme (50 mg/mL) with 0.02 M 1-ethyl-3-(3-dimethylaminopropyl) carbodiimide (EDC) and 0.02 M NHS for 3 h. The enzyme immobilized electrode was rinsed with phosphate buffer solution (pH 7.0) to remove the excess unbound enzyme (Fig. 1B). All experiments were carried out at room temperature. The enzyme immobilized electrode was stored under dry conditions at 4 °C in a refrigerator.

2.5. Characterization

Electrochemical measurements of the electrodes were carried out on a Potentiostat/Glavanostat (Princeton Applied Research, Versa Stat3) unit with three electrodes in a 50 mM phosphate buffer

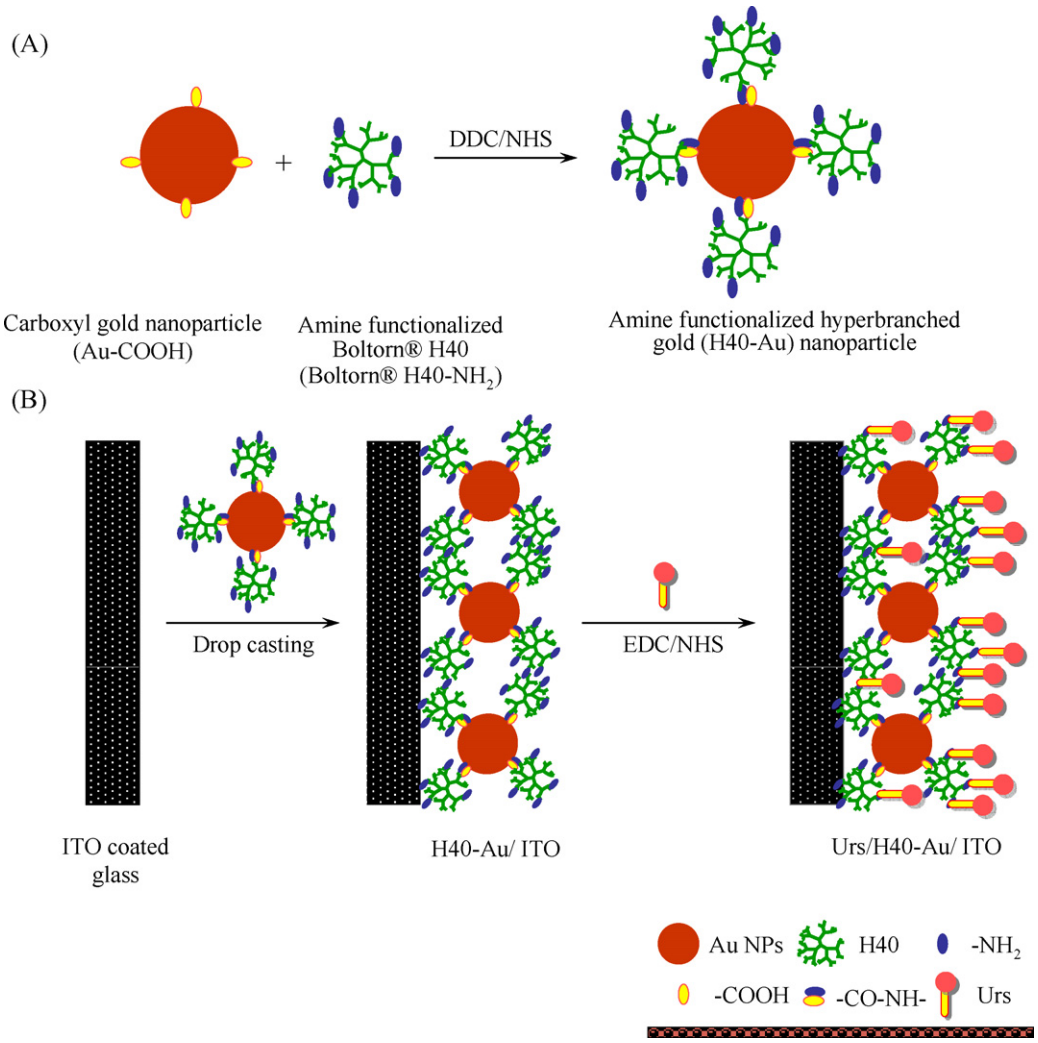

Fig. 1. Schematic presentation of the [A] preparation of hyperbranched gold (H40–Au) nanoparticles and [B] fabrication of H40–Au/ITO and Urs/H40–Au/ITO electrodes.

solution (pH 7.0, 0.9% NaCl) containing 0.5 mM hematein. The working electrode was either H40–Au/ITO or Urs/H40–Au/ITO. Platinum foil and Ag/AgCl were used as the counter and reference electrodes, respectively.

Photometric study was performed using a Varian Cary 100 Bio UV-visible spectrophotometer. For photometric measurements, a Urs/H40–Au/ITO electrode was dipped in a 5 mL phosphate buffer solution (50 mM, pH 7.0), which contained 200 μL of Nessler's solution and 1 mL of urea solution with varying concentrations. After 2 min of Urs/H40–Au/ITO electrode incubation, the absorbance of the colored product (i.e., $NH_2Hg_2I_3$, a complex formed between the Nessler's reagent and ammonia produced by the enzymatic hydrolysis of urea) in the solution at λ_{max} 385 nm, was measured to monitor the Urs enzyme kinetics.

FTIR spectra were recorded on a Perkin Elmer, Spectrum BX-II spectrophotometer. The surface morphology of the electrodes was examined with a Hitachi S-4800 field emission scanning electron microscope (SEM) operated at 5 kV. The specimens were sputter-coated with a thin layer of iridium (~5 nm) prior to examination. The morphology of H40–Au nanoparticles was further studied by transmission electron microscopy (TEM, Hitachi H-600) operated at 75 kV. A TEM sample was prepared by depositing 6 μL solution of H40–Au (ultrasonically dispersed in THF) on a copper grid coated with formbar and a carbon film using phosphotungstic acid (PTA) as a negative staining agent. All measurements were carried out at 20 °C.

3. Results and discussion

3.1. Electrode fabrication and characterization

The H40–NH_2 grafted Au–COOH nanoparticles were prepared via the formation of amide bonds between the amine groups of H40–NH_2 and the carboxylic acid group of Au–COOH. The resulting H40–Au nanoparticles were deposited onto an ITO coated glass substrate to form a uniform film. The free amino groups still present in the H40–Au nanoparticles were further used for covalent immobilization of Urs using NHS and EDC as the coupling agents during the bioelectrode preparation process [9]. Fig. 1 shows the overall steps for preparing H40–Au nanoparticles and fabricating the H40–Au/ITO and Urs/H40–Au/ITO electrodes.

The resultant enzyme immobilized electrode was characterized by FTIR spectroscopy. Fig. 2 shows the FTIR spectra of the H40–Au/ITO and Urs/H40–Au/ITO electrodes. The FTIR spectrum of the H40–Au/ITO electrode (Fig. 2A) showed the characteristic peaks at: (1) 3117–3281 cm^{-1} (O–H and N–H stretching); (2) 2946 and 2881 cm^{-1} (C–H stretching of $-CH_2$ groups); (3) 1731 cm^{-1} (C=O stretching of ester group); and (4) 1639 cm^{-1} (C=O stretching of amide group). The C=O characteristic peaks at 1639 cm^{-1} confirms the formation of amide bonds between H40–NH_2 and Au–COOH nanoparticles. In addition, the absorption band at 3117–3281 cm^{-1} indicates the presence of residual amino groups on the H40–Au nanoparticles that are used to immobilize the Urs.

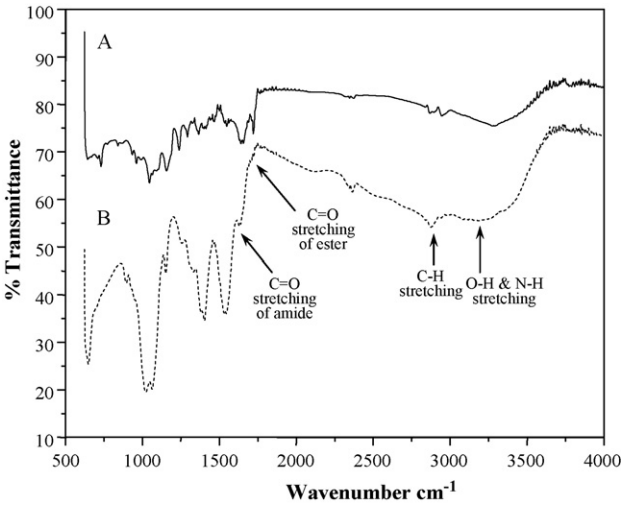

Fig. 2. FTIR spectra of the [A] H40–Au/ITO and [B] Urs/H40–Au/ITO electrodes.

The FTIR spectrum of the Urs/H40–Au/ITO electrode (Fig. 2B) showed peaks broadening at (1) 3067–3330 cm^{-1} (N–H stretching vibration); (2) 2930–2872 cm^{-1} (C–H stretching of $–CH_2$ groups); and (3) 1633 cm^{-1} (C=O stretching of amide group) due to the attachment of Urs enzyme through the peptide linkage on the electrode. Hence, FTIR spectra confirm the covalent immobilization of Urs onto the H40–Au/ITO electrode.

A typical SEM picture of H40–Au/ITO (Fig. 3A) exhibited tiny H40–Au particles with a porous surface. The nanoporous surface of the H40–Au/ITO electrode provided a very high surface-to-volume ratio, which can enhance the interaction between Urs and the H40–Au film of the electrode. Consequently, this will lead to a much higher level of enzyme stability and much better enzyme reproducibility for the Urs/H40–Au/ITO electrode. Immobilization of the Urs enzyme over the H40–Au/ITO electrode surface produced a homogeneous dentritic surface morphology (Fig. 3B). The uniform dentritic-like enzyme electrode surface may be formed due to the covalent binding of Urs molecules over the gold nanoparticles functionalized with hyperbranched polyester, i.e., the H40–Au nanoparticles.

To further understand the morphology of the H40–Au nanoparticles, TEM analysis was conducted using PTA as a staining agent (Fig. 3C). As demonstrated in Fig. 1A, multiple hyperbranched H40–NH_2 polyester molecules may be grafted onto one Au–COOH nanoparticle by amide bonds. The average size of the resulting H40–Au nanoparticles was 16 nm according to the TEM analysis. The PTA stain clearly showed the light contrast of hyperbranched H40–NH_2 molecules/nanoparticles and the dark contrast of Au–COOH nanoparticles with an average size of 3 and 12 nm, respectively. The size of the H40–NH_2 molecules/nanoparticles detected here is consistent with the average size of Boltron® H40 molecules/nanoparticles (i.e., 3 nm) reported in the literature [35]. The TEM image of the H40–Au nanoparticles clearly showed the formation of hyperbranched H40–NH_2 functionalized gold nanoparticles.

3.2. Amperometric measurements

Fig. 4 shows the CVs of the electrochemical cells using either H40–Au/ITO or Urs/H40–Au/ITO electrode at a constant 50 mV s^{-1} scan rate in 50 mM phosphate buffer solution (pH 7.0, 0.9% NaCl) containing 0.5 mM hematein. The current of the electrochemical cell using the Urs/H40–Au/ITO electrode (2.1×10^{-4} A) was about one-half of that using the H40–Au/ITO electrode (3.9×10^{-4} A). Thus, immobilizing Urs onto the electrode reduced the current. A decrease in current after the immobilization of Urs may be attributed to a slower redox behavior when compared with the bare H40–Au/ITO electrode. The covalent binding of Urs on the H40–Au/ITO electrode controls the moment of the supporting electrolytes [36]. Also, the non-conducting nature of the Urs molecules might have contributed to the decrease in current when using the Urs/H40–Au/ITO electrode.

Amperometric measurements were carried out with the Urs/H40–Au/ITO electrode for quantitative determination of urea in an aqueous medium using hematein, a pH-sensitive natural dye

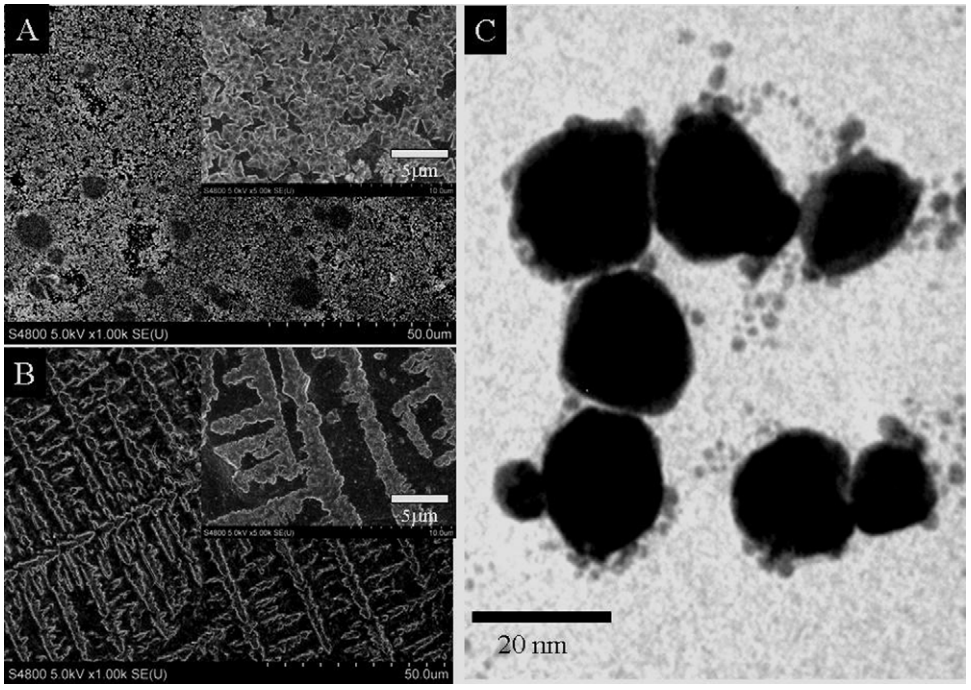

Fig. 3. Electron microscopic study of the [A] H40–Au/ITO using SEM, [B] Urs/H40–Au/ITO using SEM, and [C] hyperbranched H40–Au nanoparticles using TEM.

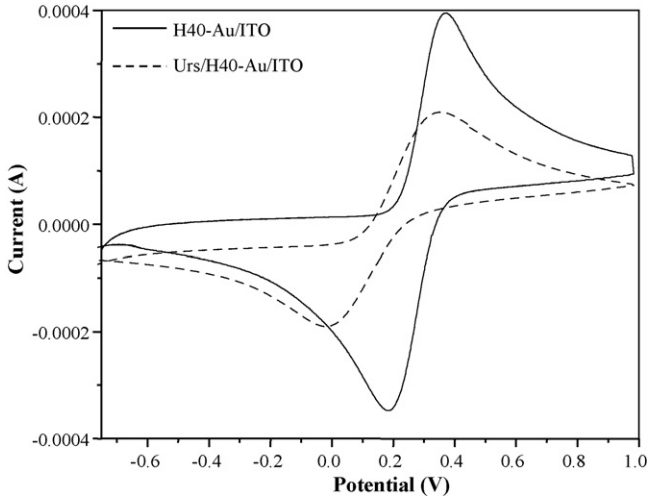

Fig. 4. Cyclic voltammograms of the [A] H40–Au/ITO and [B] Urs/H40–Au/ITO electrodes in 50 mM phosphate buffer solution at pH 7.0 containing 0.9% NaCl and 0.5 mM hematein.

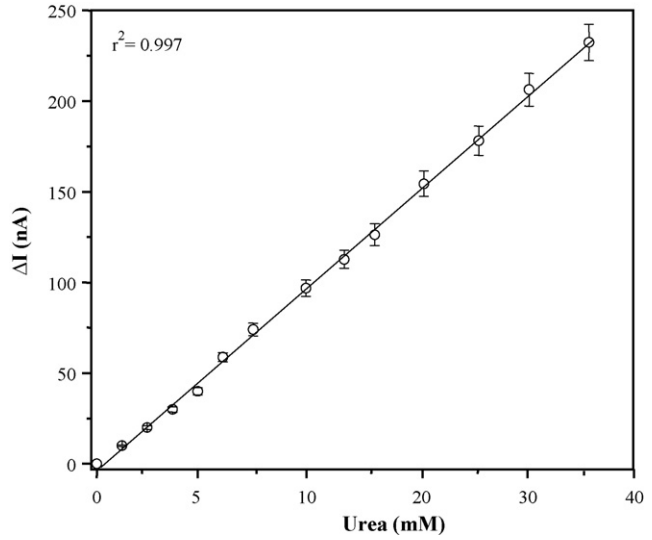

Fig. 5. Amperometric response of Urs/H40–Au/ITO bioelectrode with the urea concentration ranging from 0.01 to 35 mM at working potential of 0 mV vs. Ag/AgCl using 50 mM phosphate buffer solution containing 0.9% NaCl and 0.5 mM hematein.

[37]. Cyclic voltammetric studies were carried out in 50 mM phosphate buffer solution containing 0.5 mM hematein and 0.9% NaCl. It was observed that the cathodic peak shifted to a more positive potential as the pH value decreased. The shift in the cathodic peak potential was approximately 29 mV per pH unit. Previous studies indicated the stability of hematein in electrochemical cells using Pt and graphite composite electrodes depended on both pH and the applied voltage [37,38]. Thus, to avoid electrochemical interference on the stability of hematein, an amperometric measurement of urea should be conducted at a working potential of 0 mV [37].

Fig. 5 shows the steady-state current dependence calibration curve for the urea concentration ranging from 0.01 to 35 mM. An amperometric linear response ($r^2 = 0.997$) was observed with the successive addition of urea to the phosphate buffer solution containing 0.9% NaCl as the electrolyte and 0.5 mM hematein as the redox indicator under a constant stirring of 100 rpm at 2-min intervals. The electrode responded within 3 s to the change of urea concentration. The current sensitivity of the enzyme electrode toward urea concentrations was 7.48 nA/mM. This new type of urea

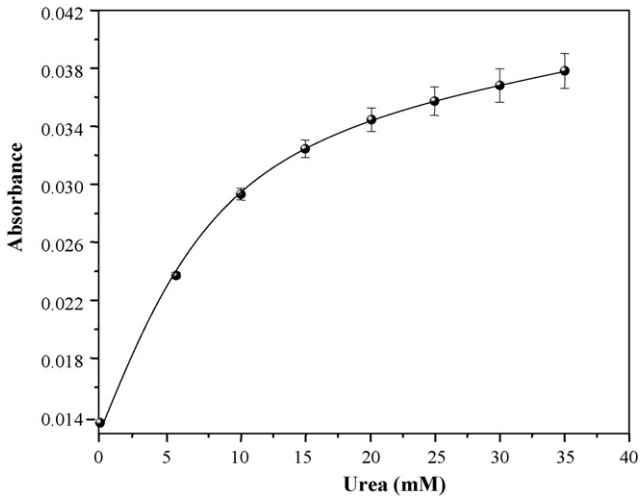

Fig. 6. Photometric response as a function of urea concentration ranging from 0.01 to 35 mM using a Urs/H40–Au/ITO electrode exposed with an equal amount of Nessler's reagent.

biosensor demonstrated a shorter response time and a broader detection range compared with those reported previously, as shown in Table 1. Table 1 provides the comparison of the performance of this new type of urea biosensor with those reported previously and will be further discussed later.

The affinity of Urs to the urea was estimated using the Hanes plot [39]. The Michaelis–Menten kinetic parameter (K_m^{app}) was calculated to be 0.96 mM for the Urs/H40–Au/ITO electrode. K_m^{app} usually depends on the electrode material as well as the enzyme immobilization process [40]. The K_m^{app} of the biosensor using Urs/H40–Au/ITO as the electrode is much less than that of these previously reported biosensors (typically 2–7 mM) [41,6]. The small K_m^{app} value indicates a high affinity of Urs to the urea over the Urs/H40–Au/ITO electrode surface, which may be attributed to (1) the advantageous nanoporous surface of the H40–Au/ITO electrode for the enzyme immobilization that can favor conformational changes of the enzyme and (2) the high surface-to-volume ratio, which can help to effectively immobilize Urs onto the H40–Au/ITO electrode. In addition, functionalized H40–Au nanoparticles can provide efficient electron transfer between the active site of the enzyme and the electrode, thereby enhancing the urea sensing activity.

3.3. Photometric study

A photometric response study was performed to calculate the apparent enzyme activity of the Urs/H40–Au/ITO electrode. Urs catalyzes the hydrolysis of urea to produce ammonia, which in turn reacts with the Nessler's reagent to form a colored product, $NH_2Hg_2I_3$ [42]. By following the absorbance of $NH_2Hg_2I_3$ at 385 nm, urea can be quantified and the analytical performance of the biosensor can be determined. The difference between the initial and final absorbance value at 385 nm were plotted as a function of urea concentration, as shown in Fig. 6. The enzyme electrode responded to the urea concentration within the range of 0.01–35 mM. The apparent enzyme activity ($^{enz}a_{app}$) was calculated using equation $^{enz}a_{app} = AV/\varepsilon ts$, where A is the difference in absorbance before and after incubation, V is the total volume of the solution, ε is the millimolar extinction coefficient, t is the reaction time and s is the surface area of the electrode. The apparent enzyme activity was calculated to be 71.59 mg/cm^2, indicating 71.59 mg of Urs was actively working per unit area of electrode surface.

Table 1
Assessment of the Urs/H40–Au/ITO biosensor characteristics with other previously reported amperometric urea biosensors.

Sl. No.	Electrode material	Immobilization method	Stability	Linear range	Detection limit	Response time	Reference
1.	Nylon net	Encapsulation	4 days	$0.1–3 \times 10^{-4}$ M	10^{-5} M	–	[44]
2.	Graphite and platinum composite	Physical adsorption	90 days	$1–25 \times 10^{-5}$ M	1×10^{-5} M	120 s	[37]
3.	Polyaniline-Nafion/Au/ceramic composite	Covalent	–	6–60 mg/dL	0.3 mg/dL	–	[18]
4.	Poly(*N*-3-aminopropyl pyrrole-*co*-pyrrole)	Covalent	60 days	$0.16–5.02 \times 10^{-5}$ M	0.16×10^{-5} M	40 s	[17]
5.	Poly(vinylferrocium)	Ionic binding	29 days	$1–25 \times 10^{-5}$ M	1×10^{-6} M	60 s	[45]
6.	Functionalized H40–Au nanoparticles	Covalent	126 days	$1–3500 \times 10^{-5}$ M	1×10^{-5} M	3 s	Present work

Table 2
Evaluation of the present method with the spectrophotometric method for the determination of urea from human blood serum and urine.

Sample no.	Urea concentration		% Error
	Present method	Standard spectrophotometric method	
Blood serum sample-1	2.8 ± 0.01 mM	2.6 ± 0.015 mM	7.14
Blood serum sample-2	3.4 ± 0.01 mM	3.1 ± 0.015 mM	8.82
Urine sample-1	316.2 ± 0.01 mM	309.4 ± 0.015 mM	2.19
Urine sample-2	274.9 ± 0.01 mM	262.7 ± 0.015 mM	4.64

3.4. Reproducibility and accuracy

The lowest detection limit of the urea electrode was 0.01 mM. The reproducibility of the response of the enzyme electrode was investigated at a 5 mM urea concentration. No significant decrease in current response was observed after at least 10 uses in testing; thus, the enzyme electrode displayed good reproducibility. The relative standard deviation was found to be about 8% determined by five successive measurements of a 5 mM urea standard using a single biosensor with the same Urs/H40–Au/ITO electrode. In a series of 10 biosensors using 10 different Urs/H40–Au/ITO electrodes, a relative standard deviation of about 6% was obtained for the individual current response of the same sample (5 mM urea). The good reproducibility observed with the biosensor may be attributed to the efficient bonding of the enzyme with the functionalized H40–Au nanoparticles.

3.5. Thermal stability

The thermal stability of the Urs/H40–Au/ITO electrode was studied by measuring the current at different temperatures ranging from 20 to 45 °C in the presence of 5 mM urea. It was observed that the reaction rate increased with the temperature up to 30 °C and the optimum temperature range was between 28 and 30 °C due to the increased kinetic energy of the reacting molecules. The storage stability of the Urs/H40–Au/ITO electrode was amperometrically measured and a similar current response was found after storing for 18 weeks at 4 °C.

3.6. Interference study

The effect of interferents was studied on the amperometric responses of the biosensor employing the Urs/H40–Au/ITO electrode in the presence of 5 mM urea. The interference effects of L-serine, L-threonine, α-ketoglutaric acid, L-alanine, L-phenylalanine, uric acid, L-cystine, L (+)-glutamic acid, sodium pyruvate, L-glutamine, and L-ascorbic acid was investigated by measuring the amperometric response of the Urs/H40–Au/ITO electrode. These substances were added into the reaction mixture at their normal physical concentration, i.e., 0.2 mM. It was found that the presence of interferents had a relative error of less than 4% in the current measured by the amperometric method; therefore, this bioelectrode can detect urea with negligible interference.

3.7. Performance of biosensor with biological samples

To demonstrate the feasibility of the Urs/H40–Au/ITO biosensor for urea analysis, samples of fresh blood serum and urine from a healthy person were analyzed. The analyses were performed without any sample pretreatment and results were compared with those obtained from the standard spectrophotometric method [43]. As shown in Table 2, the value of urea concentration in blood serum and urine obtained with Urs/H40–Au/ITO biosensor was ~2–9% higher than those obtained from the standard method [43], most

likely due to the interferences of the electroactive species present in blood plasma and urine. Overall, a good agreement of the urea concentration in both cases was observed.

Table 1 compares the characteristics of the new amperometric urea biosensor based on the Urs/H40–Au/ITO electrode with those reported in the literature. It is apparent that the Urs/H40–Au/ITO based urea biosensor exhibited a longer shelf life, higher sensitivity, wider range of detection limit, and shorter response time.

4. Conclusion

A new type of urea biosensor based on a Urs/H40–Au/ITO bioelectrode was successfully fabricated and evaluated. Urs was covalently immobilized onto the nanoporous film formed by gold nanoparticles functionalized with hyperbranched Boltron® H40 polyester on the ITO coated glass (H40–Au/ITO). The H40–Au/ITO electrode surface offered a high level of enzyme immobilization leading to a highly stable Urs/H40–Au/ITO bioelectrode. The urea biosensor showed a linear current response to the urea concentration ranging from 0.01 to 35 mM and it exhibited a sensitivity of 7.48 nA/mM with a response time of 3 s. The relatively low Michaelis–Menten constant of 0.96 mM indicates that the H40–Au/ITO electrode surface had a high affinity for the Urs enzyme. This new type of urea biosensor has demonstrated superior performance compared with those reported previously, including a longer shelf life, higher sensitivity, wider range of detection limit, and shorter response time.

Acknowledgement

The authors would like to acknowledge the financial support to carry out this work from National Science Foundation (NSF), USA under the project CMMI-0734881.

References

[1] A.C. Guyton, Science 252 (1991) 1813.
[2] D. Aronson, Am. J. Med. 116 (2004) 466.
[3] C. Ronco, R. Bellomo, P. Homel, A. Brendolan, M. Dan, P. Piccinni, G.L. Greca, Lancet 355 (2000) 26.
[4] D.H. Yun, M.J. Song, S.I. Hong, J. Korean Phys. Soc. 47 (2005) S445.
[5] W.J. Cho, H.J. Huang, Anal. Chem. 70 (1998) 3946.
[6] C. Eggenstein, M. Borchardt, C. Diekmann, B. Grundig, C. Dumschat, K. Cammann, E.M.I.M. Ekanayake, D.M.G. Preethichandra, K. Kaneto, Biosens. Bioelectron. 23 (2007) 107.
[7] A.Q. Contractor, T.N. Sureshkumar, R. Narayanan, S. Sukeerthi, R. Lal, R.S. Srinavasa, Electrochim. Acta 39 (1994) 1321.
[8] A. Ramsing, J. Ruzicka, E.H. Hansen, Anal. Chim. Acta 114 (1980) 165.
[9] A. Riklin, E. Katz, I. Willner, A. Stocker, A.F. Buckmann, Nature 376 (1995) 672.
[10] B. Xie, U. Harborn, M. Mecklenburg, B. Danielsson, Clin. Chem. 40 (1994) 2282.
[11] Z. Yang, S. Si, H. Dai, C. Zhang, Biosens. Bioelectron. 22 (2007) 3283.
[12] A. Tiwari, S. Gong, Electroanalysis 20 (2008) 2119.
[13] S.B. Adeloju, S.J. Shaw, G.G. Wallace, Anal. Chim. Acta 341 (1997) 155.
[14] S.K. Jha, A. Topkar, S.F. D'Souza, J. Biochem. Biophys. Methods 70 (2008) 1145.
[15] X. Wang, H. Watanabe, N. Sekioka, H. Hamana, S. Uchiyama, Electroanalysis 19 (2007) 1300.
[16] F. Kuralay, H. Ozyoruk, A. Yıldız, Sens. Actuators B: Chem. 109 (2005) 194.
[17] Rajesh V. Bisht, W. Takashima, K. Kaneto, Biomaterials 26 (2005) 3683.
[18] Y.C. Luo, J.S. Do, Biosens. Bioelectron. 20 (2004) 15.
[19] B. Lakard, G. Herlem, S. Lakard, A. Antoniou, B. Fahys, Biosens. Bioelectron. 19 (2004) 1641.
[20] R. Singhal, A. Gambhir, M.K. Pandey, S. Annapoorni, B.D. Malhotra, Biosens. Bioelectron. 17 (2002) 697.
[21] M.M.C. Ortega, D.E. Rodriguez, J.C. Encinas, M. Plascencia, F.A.M. Velarde, R. Olayo, Sens. Actuators B: Chem. 85 (2002) 19.
[22] J.M.C.S. Magalhaes, A.A.S.C. Machado, Talanta 47 (1998) 183.
[23] A. Tiwari, S. Gong, Electroanalysis 20 (2008) 1775.
[24] J.D. Swalen, D.L. Allara, J.D. Andrade, E.A. Chandross, S. Graoff, J. Israelachvili, T.J. McCarthy, R. Murray, R.F. Pease, J.F. Rabolt, K.J. Wynne, H. Yu, Langmuir 3 (1987) 932.
[25] T. Wink, S.J. van Zuilen, A. Bult, W.P. Bennekom, Analyst 122 (1997) 43R.
[26] K. Habermuller, M. Mosbach, W. Schuhmann, Fresenius' J. Anal. Chem. 366 (2000) 560.
[27] Y. Xiao, H.X. Ju, H.Y. Chen, Anal. Biochem. 278 (2000) 22.
[28] Z. Cao, X. Jiang, Q. Xie, S. Yao, Biosens. Bioelectron. 24 (2008) 222.
[29] J.F. Hicks, F.P. Zamborini, A.J. Osisek, R.W. Murray, J. Am. Chem. Soc. 123 (2001) 7048.
[30] A.N. Shipway, M. Lahav, I. Willner, Adv. Mater. 12 (2000) 993.
[31] R. Polsky, R. Gill, L. Kaganovsky, I. Willner, Anal. Chem. 78 (2006) 2268.
[32] K.R. Brown, A.P. Fox, M.J. Natan, J. Am. Chem. Soc. 118 (1996) 1154.
[33] Y. Xiao, H.X. Ju, H.Y. Chen, Anal. Chim. Acta 391 (1999) 73.
[34] M. Prabaharan, J.J. Grailer, D.A. Steeber, S. Gong, Macromol. Biosci. 8 (2008) 843.
[35] E. Zagar, M. Zigon, J. Chromatogr. A 1034 (2004) 77.
[36] A. Tiwari, S. Gong, Talanta 77 (2009) 1217.
[37] A. Pizzariello, M. Stredansky, S. Stredanka, S. Miertus, Talanta 54 (2001) 763.
[38] M. Stredansky, A. Pizzariello, S. Stredanka, S. Miertus, Anal. Chim. Acta 415 (2000) 151.
[39] J.M. Walker, Principles, Techniques of Practical Biochemistry, 5th ed., Cambridge University Press, UK, 2000.
[40] G.K. Kouassi, J. Irudayaraj, G. McCarty, J. Nanobiotechnol. 3 (2005) 1.
[41] J.X. Wang, X.W. Sun, A. Wei, Y. Lei, X.P. Cai, C.M. Li, Z.L. Dong, Appl. Phys. Lett. 88 (2006) 233106.
[42] Rajesh V. Bisht, W. Takashima, K. Kaneto, Surf. Coat. Technol. 198 (2005) 231.
[43] F.K. Fawcett, J.E. Scott, J. Clin. Pathol. 13 (1960) 156.
[44] P. Bertocchi, D. Compagnone, G. Palleschi, Biosens. Bioelectron. 11 (1996) 1.
[45] F. Kuralay, H. Ozyoruk, A. Yildiz, Sens. Actuators B: Chem. 114 (2006) 500.